Optimization of the Power-to-Velocity Ratio in the Downlink of Vehicular Networks

Long Zhao, *Member, IEEE*, Ping Zhang, Kan Zheng, *SM, IEEE*, and Hanzo Lajos, *Life Fellow, IEEE*

***Abstract*—Consider a base station (BS) relying on a massive antenna array, which transmits information to multiple vehicles of vehicular networks. In order to jointly consider both the communication resource consumption and the road-traffic efficiency, we define a metric given by the BS's downlink power normalized by the vehicular velocity. We refer to it as the Power to Velocity Ratio (PVR). The prime objective of this paper is to minimize either the maximum individual vehicle PVR or the entire system's PVR by optimizing the power allocation at the BS, while guaranteeing the information requirements of the vehicles both under the total transmit power constraint and driving velocity constraint. As for the individual vehicle PVR, a closed-form power allocation expression is derived by assuming that the transmit power constraint is non-restrictive. Based on this an optimal power allocation algorithm is proposed for arbitrary finite transmit power constraints. As for the system PVR, the non-convex problem formulated is first transformed into a convex problem and then the optimal solution is found by conceiving an efficient iterative algorithm. Our simulation results show that the proposed algorithms indeed succeed in achieving the optimal individual vehicle or system PVR.**

***Index Terms*—Vehicular networks, power consumption, traffic efficiency.**

I. Introduction

Next-generation (NG) wireless networks are expected to support a wide variety of both conventional communications services and of emerging vertical industrial services [1]. The three typical application scenarios of NG networks include enhanced mobile broadband (eMBB), massive machine type communications (mMTC), and ultra-reliable low latency communications (uRLLC) [2]. Among many exciting applications, an important one is the seamless integration with and support of vehicular networks [2], [3] for improving the transportation efficiency, traffic safety and the quality of information services on the move [4]–[6]. In order to achieve these ambitious objectives, many recent studies have investigated the architectures and key transmission technologies of NG vehicular networks.

By combining the advantages of both dedicated short range communications (DSRC) and of the 4G long-term evolution (LTE) systems, heterogeneous vehicular network architectures were designed to support the vehicle-to-everything (V2X) scenario relying on software-defined networking (SDN) [7], [8]. To fully exploit both the communications and computing resources of vehicular networks, a triple-layer cloud (vehicular cloud, local cloud, and remote cloud) architecture was proposed for meeting the latency and complexity constraints of the associated computing tasks [8]. In this spirit, by leveraging unmanned aerial vehicles (UAV) and/or satellites, a software defined space-air-ground integrated network (SAGIN) architecture was proposed for vehicular networks in order to improve the V2X connectivity, by filling in the existing coverage holes and hence to improve the interworking efficiency [9], [10].

Indeed, rich suite of communications and networking schemes have also been developed for vehicular networks [11]- [21]. Given the growing demand for mobile data services in vehicle-to-infrastructure (V2I) communications, high-throughput non-orthogonal multiple access (NOMA) was proposed for vehicular small-cell networks to improve their spectrum and energy efficiency (EE) [11]–[14]. For the timely provision of V2I infotainment services, edge caching techniques were advocated in [15]–[17]. For vehicle-to-vehicle (V2V) communications, efficient centralized resource allocation schemes were proposed both for time-division and frequency-division multiple access [18]. In [19], a coded slotted ALOHA (CSA) scheme was conceived for distributed resource allocation in V2V communications. As a further development, cooperative schemes were proposed for vehicular networks by combining V2V and V2I communications [20], [21]. To support the video streaming services of vehicular users, a cooperative downloading mechanism was proposed for heterogeneous vehicular networks in [20]. As a recent advance, a cluster-based uplink transmission scheme was designed in [21] for improving both the latency and the throughput of vehicular networks.

In order to support the efficient management of road-traffic, the vehicular flow rate, both the vehicle density and vehicular velocity have to be accurately monitored [22]–[27]. By analyzing the inter-arrival time and speed distribution of vehicles, the associated connection characteristics and routing characteristics were investigated in [23]. The packet delivery delay of vehicular networks was analyzed in [24] in terms of the vehicle density and velocity. By taking into account both the vehicle density and channel state information (CSI), a jointly optimized resource allocation scheme was proposed in [25] for improving the latency of vehicular networks. By analyzing realistic vehicular traces and communication connections, a dynamically evolving networking model was

This work was supported in part by the China Natural Science Funding under Grant 61731004, the Engineering and Physical Sciences Research Council projects EP/P034284/1 and EP/P003990/1 (COALESCE) as well as of the European Research Council's Advanced Fellow Grant QuantCom (Grant No. 789028).

L. Zhao, P. Zhang, and K. Zheng are with the Key Lab of Universal Wireless Communications, Ministry of Education, Beijing University of Posts and Telecommunications (BUPT), Beijing, 100876, China (e-mail: z-long, zhang_ping, zkan@bupt.edu.cn).

L. Hanzo is with the School of Electronics and Computer Science, University of Southampton, Southampton SO17 1BJ, U.K. (e-mail: lh@ecs.soton.ac.uk).

proposed and the analytical expression of the graph-theoretic degree distribution was derived in [27], [28]. However, there is a paucity of literature on jointly optimizing the communication resource efficiency and road-traffic efficiency of vehicular networks.

To fill this knowledge-gap is the main inspiration of this treatise. We consider the downlink of a single-cell vehicular communication system, where a base station (BS) employing massive multiple-input multiple-output (MIMO) techniques simultaneously serves multiple vehicles within its coverage area. In this scenario, our main contributions are boldly and explicitly contrasted to the state-of-the-art in Table I, which are further detailed below:

- In order to jointly characterize the road-traffic efficiency and communication resource efficiency, a metric is defined, which is reminiscent of EE [29]–[33][1]. Explicitly, it is defined as the power consumption of the BS dedicated either to an individual vehicle or to the entire system which is normalized by the vehicular velocity, and it is referred to as the Power-to-Velocity Ratio (PVR).
- For guaranteeing the transmission rate requirements of the vehicles, as well as for optimizing the power allocation under the associated total transmit power and maximum driving velocity constraints, we solve the minimization problems of the maximum individual vehicular PVR and system PVR.
- For the minimization problem of the maximum vehicular PVR, the closed-form expression of the optimal power allocation is first derived without considering the total transmit power constraint; based on these three power allocation scenarios are then analyzed theoretically, and an efficient power allocation algorithm is proposed for minimizing the maximum vehicular PVR.
- For the minimization problem of the total system PVR, the resultant non-convex problem is first transformed into a convex form, and then an iterative power allocation algorithm is conceived for minimizing the system's PVR.
- The asymptotic analysis of the individual vehicle's PVR or the system's PVR is carried out for both high and low transmit powers. The consistency of the both these optimal power allocation schemes is proved for the pair of problems formulated in the high transmit power region.

The remainder of this paper is organized as follows. Section II describes our system model and formulates a pair of PVR minimization problems. First the problem of the individual vehicle's PVR is analyzed in Section III. Then, Section IV studies the problem formulated for the overall system's PVR and the optimal solution is derived. Finally, Section V presents our simulation results, while our concluding remarks are offered in Section VI.

Notations: Uppercase and lowercase boldface letters denote matrices and vectors, respectively; $(\cdot)^{\mathrm{T}}$ and $(\cdot)^{*}$ represent the transpose and conjugate of a matrix/vector, respectively; The constant e is the base of natural logarithms; $\|\cdot\|$ refers to the Euclidean norm; $\mathbb{N}\left(\mu,\sigma^2\right)$ denotes the real-valued Gaussian distribution with mean μ and variance σ^2; $\mathbb{CN}\left(\mu,\sigma^2\right)$ is the complex-valued Gaussian distribution with mean μ and real/imaginary component variance of $\sigma^2/2$. $[x]_a^b = \max\{\min\{x,b\},a\}$ and $[x]^+ = \max\{x,0\}$.

[1]In the specific scenario, when the vehicular velocity is proportional to the information transmission rate, the PVR metric becomes reminiscent of the concept of EE with a unit of J/bit, as observed in the proof of *Theorem 1* given in Appendix A. This special case is also convenient in terms of providing a plausible physical interpretation.

II. System Model and Problem Formulation

A. System Model

As illustrated in Fig. 1, a BS equipped with M transmit antennas simultaneously transmits the position-related information to K single-antenna vehicles (labeled as $\mathcal{K} = \{1,2,\cdots,K\}$) travelling on the road considered. The vehicular system is assumed to operate in a time division duplex (TDD) mode and the system bandwidth is B Hz. The position-related information volume m can be calculated in terms of bits per meter (bit/m), including the high-definition (HD) map representing the driving-related environment versus the position information [34][35]. To elaborate a little further, the extra position-related information overhead of q_k $(k \in \mathcal{K})$ (in units of bit/s) should be taken into account. Given the velocity v_k of the kth vehicle, the associated overhead rate should satisfy $mv_k + q_k \leq r_k$.

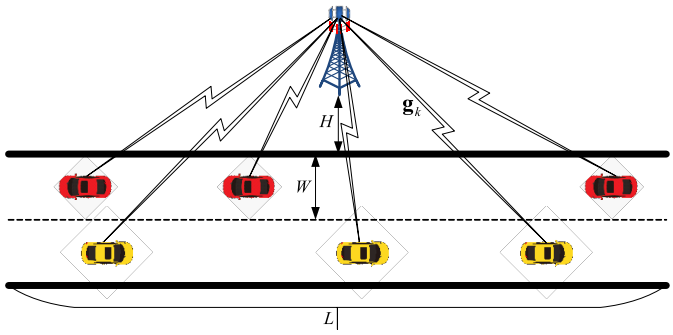

Fig. 1. Illustration of the information transmission scenario considered.

1) Channel Model: Block fading channels are assumed, where the complex envelope remains constant within a coherence time interval and changes randomly between blocks.

Let us denote the channel vector spanning from the BS to the kth vehicle by $\mathbf{g}_k^{\mathrm{T}} = \delta_k^{1/2}\mathbf{h}_k^{\mathrm{T}}$, where δ_k represents the large-scale fading coefficient that incorporates both the path loss and shadowing effects. Furthermore, $\mathbf{h}_k = [h_{k1}, h_{k2}, \cdots, h_{kM}]^{\mathrm{T}}$ contains independent and identically distributed (i.i.d.) complex Gaussian distributed elements with zero mean and unit variance [36]. In other words, Rayleigh fading channels are assumed to reflect the ultimate worst-case fading based theoretical performance that can be achieved by the system without considering the entire suite of implementation-specific aspects under diverse Rician conditions; Rician fading channels may also be considered in practical systems [37], [38] and the beam-domain transmission aspects [39], [40] may also be studied in our future research.

Based on the transmitted orthogonal pilot sequences of vehicles within a coherence time interval, the BS can estimate

TABLE I
THE STATE-OF-THE-ART OF VEHICULAR COMMUNICATIONS.

Key words	Our paper	[14] 2020	[15] 2018	[16] 2019	[17] 2020	[18] 2016	[19] 2017	[20] 2018	[21] 2015	[22] 2018	[23] 2007	[24] 2011	[25] 2020	[26] 2012	[27] 2020
V2I	√	√	√	√	√	√	√	√	√				√		
V2V						√	√	√	√	√	√	√		√	√
Estimated CSI	√												√		
Beamforming	√												√		
Data rate	√	√		√	√			√	√			√	√		
Latency		√	√		√	√		√	√			√	√		
PVR	√														
Road-traffic	√		√	√	√		√	√	√	√	√	√	√	√	√
Velocity guidance	√														
Power allocation	√	√											√		

the uplink channel $\hat{\mathbf{h}}_k\,(k\in\mathcal{K})$, and then obtain the downlink channels $\hat{\mathbf{h}}_k^{\mathrm{T}}\,(k\in\mathcal{K})$ by exploiting the channel's reciprocity in TDD systems. Moreover, by considering minimum mean square error (MMSE) channel estimation, we can assume that

$$\mathbf{h}_k=\sqrt{\theta_k}\hat{\mathbf{h}}_k+\sqrt{1-\theta_k}\mathbf{e}_k,\ k\in\mathcal{K}, \tag{1}$$

where the estimated channel $\hat{\mathbf{h}}_k\sim\mathbb{CN}\left(\mathbf{0},\mathbf{I}_M\right)$ is independent of the channel error $\mathbf{e}_k\sim\mathbb{CN}\left(\mathbf{0},\mathbf{I}_M\right)$ of $\mathbf{h}_k$, and $\theta_k\in[0,1]$ determines the channel estimation accuracy [41], [42].

2) Downlink Signal Transmission: In the massive MIMO downlink, the matched-filter (MF) based beamformers can be formulated as

$$\mathbf{w}_k=\hat{\mathbf{h}}_k^*\Big/\left\|\hat{\mathbf{h}}_k\right\|,\ k\in\mathcal{K}, \tag{2}$$

which have been proved to be asymptotically optimal for low-complexity information transmission [36], [41], [43]. Hence we opted for their employment in this paper. Assuming that p_k/M and that $u_k\in\mathbb{C}$ with $|u_k|=1$ represent the transmit power and the symbol transmitted to the kth vehicle by the BS, the received signal of the kth vehicle can be expressed as

$$\begin{aligned}y_k=&\mathbf{g}_k^{\mathrm{T}}\sum_{i=1}^{K}\sqrt{\frac{p_i}{M}}\mathbf{w}_iu_i+n_k\\=&\sqrt{\frac{p_k\delta_k\theta_k}{M}}\hat{\mathbf{h}}_k^{\mathrm{T}}\mathbf{w}_ku_k+\sum_{i=1,i\neq k}^{K}\sqrt{\frac{p_i\delta_k\theta_k}{M}}\hat{\mathbf{h}}_k^{\mathrm{T}}\mathbf{w}_iu_i\\&+\sum_{i=1}^{K}\sqrt{\frac{p_i\delta_k\left(1-\theta_k\right)}{M}}\mathbf{e}_k^{\mathrm{T}}\mathbf{w}_iu_i+n_k,\end{aligned} \tag{3}$$

where $n_k\sim\mathbb{CN}\left(0,N_kB\right)$ denotes the complex additive white Gaussian noise (AWGN) at the kth vehicle having the noise power spectral density of N_k.

Upon introducing $\mathbf{p}=\left[p_1,p_2,\cdots,p_K\right]^{\mathrm{T}}$, the signal-to-interference-plus-noise ratio (SINR) of the kth vehicle can be written as

$$\gamma_k\left(\mathbf{p}\right)=\frac{p_k\left|\hat{\mathbf{h}}_k^{\mathrm{T}}\mathbf{w}_k\right|^2}{\sum\limits_{i=1,\neq k}^{K}p_i\left|\hat{\mathbf{h}}_k^{\mathrm{T}}\mathbf{w}_i\right|^2+\frac{1-\theta_k}{\theta_k}\sum\limits_{i=1}^{K}p_i\left|\mathbf{e}_k^{\mathrm{T}}\mathbf{w}_i\right|^2+\frac{MN_kB}{\delta_k\theta_k}}, \tag{4}$$

and the associated information transmission rate is given by

$$r_k\left(\mathbf{p}\right)=B\log_2\left[1+\gamma_k\left(\mathbf{p}\right)\right]. \tag{5}$$

3) Power Consumption Model: Based on [44]–[46], a realistic power consumption model of the BS contains both the transmit power, $p_k/M\ \ (k\in\mathcal{K})$ dissipated by the power amplifiers (PAs) and the circuit power, p_{C}, consumed by signal processing.

The circuit power consumption, p_{C}, mainly consists of the following terms: the power dissipated by the channel coding and modulation responsible for bit-to-symbol mapping $c\sum_{k=1}^{K}r_k\left(\mathbf{p}\right)$, where c denotes the average power consumption coefficient (PCC) of coding and modulation per bit; the power dedicated to computing the MF beamformer matrix a_1K+b_1MK, where a_1 and b_1 represent the average PCCs of the complex addition and multiplication operations, respectively; the power of the active radio frequency (RF) chains b_0M, where b_0 is the average PCC of each RF link, including the D/A converter, filters, up-conversion, etc.; and the fixed power consumption a_0, which is required for BS-cooling, control signaling, and the load-independent power of baseband processors, etc. [44]–[46].

Therefore, the circuit power consumption is a function of the transmission rate, of the number of antennas and of the number of vehicles, which can be written as

$$p_{\mathrm{C}}\left(\mathbf{p}\right)=\sum_{i=0}^{1}a_iK^i+M\sum_{i=0}^{1}b_iK^i+c\sum_{k=1}^{K}r_k\left(\mathbf{p}\right). \tag{6}$$

Assuming that the vehicle-independent power terms a_0+Mb_0 are equally divided amongst the vehicles, the total power consumption of the BS for the kth vehicle can be then written as

$$p_{\mathrm{T}k}\left(\mathbf{p}\right)=\frac{\varsigma p_k}{\varphi M}+\frac{a_0+Mb_0}{K}+a_1+Mb_1+cr_k\left(\mathbf{p}\right), \tag{7}$$

where φ and ς represent the PA efficiencies and the peak to average power ratio (PAPR) at the BS, respectively [44]–[46].

B. Problem Formulation

The vehicular velocity may be adopted for characterizing the road-traffic efficiency (the other two main metrics, namely, the road-traffic density and the road-traffic flow rate, can be

expressed as functions of the velocity [47], [48]); On the other hand, the communication overhead can also be characterized by translating it into its power consumption, when the other system resources (such as bandwidth, the number of antennas) were fixed. Therefore, in order to build a bridge between the communication cost and road-traffic efficiency, the salient metric of PVR (expressed in units of Joule/m) is used for quantifying the road-traffic efficiency supported by communication. In other words, the PVR metric could also be interpreted as the energy consumption (in units of Joule) per driving distance (in meter).

Taking into account the fairness among the vehicles or the whole system performance [49], this paper will study the PVR from the perspectives of both the individual vehicles and of the entire vehicular system. Therefore, the individual vehicle's PVR and the entire system's PVR are considered next. Then the problems of minimizing both the maximum vehicle PVR and the system PVR are formulated, respectively.

1) Optimization Problem of the Individual Vehicle's PVR: Considering the metric of J/m, the vehicle PVR is defined as the power consumption of an individual vehicle divided by the distance travelled by the corresponding vehicle, formulated as:

$$\eta_k\left(\mathbf{p}, v_k\right)=\frac{p_{\mathrm{T}k}\left(\mathbf{p}\right)}{v_k}, k \in \mathcal{K}. \tag{8}$$

Limited by the maximum transmit power p_{M}/M of the BS and the maximum driving velocity v_{M} of each vehicle, as well as considering the information rate requirements of the vehicles, one of the prime objectives of this paper is to minimize the maximum PVR of the vehicles, while considering fairness among them, yielding:

$$\min_{\mathbf{p}, v_k} \max_{k}\left\{\eta_k\left(\mathbf{p}, v_k\right)\right\} \tag{9}$$

$$\text{s.t. } mv_k+q_k \leq r_k, \tag{10}$$

$$0 \leq v_k \leq v_{\mathrm{M}}, \tag{11}$$

$$\mathbf{1}^{\mathrm{T}}\mathbf{p} \leq p_{\mathrm{M}}, \tag{12}$$

$$p_k \geq 0, k \in \mathcal{K}. \tag{13}$$

2) Optimization Problem of the Entire System's PVR: Similarly, the system PVR is defined as the total (or average) power consumption of the BS divided by the total (average) distance travelled by all vehicles, formulated as:

$$\eta_{\mathrm{S}}\left(\mathbf{p}, \mathbf{v}\right)=\frac{\frac{1}{K}\sum_{k=1}^{K} p_{\mathrm{T}k}\left(\mathbf{p}\right)}{\frac{1}{K}\mathbf{1}^{\mathrm{T}}\mathbf{v}}=\frac{\sum_{k=1}^{K} p_{\mathrm{T}k}\left(\mathbf{p}\right)}{\mathbf{1}^{\mathrm{T}}\mathbf{v}}, \tag{14}$$

where the velocity vector is $\mathbf{v}=\left[v_1, v_2, \cdots, v_K\right]^{\mathrm{T}}$.

Constrained by the maximum transmit power p_{M}/M of the system and the maximum driving velocity v_{M} of each vehicle, as well as considering the information rate requirements of all vehicles, another objective of this paper is to minimize the system PVR in order to improve the overall system performance, yielding:

$$\min_{\mathbf{p}, \mathbf{v}}\left\{\eta_{\mathrm{S}}\left(\mathbf{p}, \mathbf{v}\right)\right\} \tag{15}$$

$$\text{s.t. } mv_k+q_k \leq r_k, \tag{16}$$

$$0 \leq v_k \leq v_{\mathrm{M}}, \tag{17}$$

$$\mathbf{1}^{\mathrm{T}}\mathbf{p} \leq p_{\mathrm{M}}, \tag{18}$$

$$p_k \geq 0, k \in \mathcal{K}. \tag{19}$$

By solving the pair of problems formulated, we can determine both the power allocation required for communications and the vehicle velocities to be maintained for intelligent transportation control (such as the control or guidance concerning the velocities of the unmanned or manned vehicles). Next, the optimization problems of the vehicle PVR and system PVR will be investigated in Sections III and IV, respectively.

III. Optimization of Vehicle PVR

This section first discusses the optimal PVR of each vehicle under the non-restrictive power constraint (NRPC) in (12). Based on this, an efficient power allocation algorithm is then proposed for the problems formulated in (9)–(13) by analyzing three power constraint scenarios. Moreover, in contrast to the NRPC, the asymptotic solutions are analyzed in the face of a stringent, i.e., restrictive transmit power constraint.

A. Power Allocation Under Non-Restrictive Transmit Power Constraint

When the total transmit power constraint is high enough to become non-restrictive, the constraint (12) may be ignored and then we have the following theorem.

Theorem 1: Without considering the transmit power constraint in (12) for the problems formulated in (9)–(13), the optimal driving velocity, power allocation and PVR for the kth vehicle can be written respectively as

$$\tilde{v}_k=\min\left\{\frac{B\left[W_0\left(\Psi_k\right)+1\right]}{m\ln 2}, v_{\mathrm{M}}\right\} \triangleq \min\left\{\hat{v}_k, v_{\mathrm{M}}\right\}, \tag{20}$$

$$\tilde{p}_k=\frac{BN_k}{\delta_k\theta_k}\left\{\exp\left[\frac{\ln 2}{B}\left(m\tilde{v}_k+q_k\right)\right]-1\right\}, \tag{21}$$

and

$$\tilde{\eta}_k=cm+\frac{\varsigma \mathrm{e} N_k 2^{\frac{q_k}{B}}}{\varphi M\delta_k\theta_k}\cdot\begin{cases}\frac{\left[\mathrm{e}^{W_0(\Psi_k)}+\Psi_k\right]m\ln 2}{W_0(\Psi_k)+1}, & \hat{v}_k \leq v_{\mathrm{M}},\\ \frac{B}{v_{\mathrm{M}}}\left[\mathrm{e}^{\frac{mv_{\mathrm{M}}\ln 2}{B}-1}+\Psi_k\right], & \hat{v}_k > v_{\mathrm{M}},\end{cases} \tag{22}$$

where

$$\Psi_k=\frac{\frac{\varphi M\delta_k\theta_k}{\varsigma BN_k}\left(\frac{a_0+Mb_0}{K}+a_1+Mb_1+cq_k\right)-1}{\exp\left(\frac{q_k\ln 2}{B}+1\right)}, \tag{23}$$

and $W_0\left(x\right):\left[-\mathrm{e}^{-1}, \infty\right) \rightarrow \left[-1, \infty\right)$ is the first real branch of the Lambert function satisfying $W_0\left(x\right)\mathrm{e}^{W_0(x)}=x$ [50].

Proof. Please see Appendix A. □

According to *Theorem 1*, the min-max PVR of all vehicles can be written under the NRPC scenario as:

$$\tilde{\eta} = \max_{k\in\mathcal{K}} \{\tilde{\eta}_k\}. \tag{24}$$

On the other hand, based on (51) in Appendix A, the transmit power should satisfy $p_k > p_{k\mathrm{m}} \triangleq \frac{N_k B}{\delta_k \theta_k}\left(2^{q_k/B}-1\right)$ and $p_{\mathrm{M}} > p_{\mathrm{m}} \triangleq \mathbf{1}^{\mathrm{T}}\mathbf{p}_{\mathrm{m}}$ to guarantee the solvability of the problems formulated in (9)–(13), where $\mathbf{p}_{\mathrm{m}} = [p_{1\mathrm{m}}, p_{2\mathrm{m}}, \cdots, p_{K\mathrm{m}}]^{\mathrm{T}}$.

B. Power Allocation for Arbitrary Transmit Power Constraint

In order to obtain the solution of problems in (9)–(13), we first analyze the properties of the objective function in (9). Based on these properties and on *Theorem 1*, the optimal power allocation algorithm is then formulated for minimizing the maximum PVR.

Theorem 2: The vehicle PVR function $\eta_k(p_k)$ is a convex function with respect to the allocated power p_k; Given the PVR value $\eta\,(>\tilde{\eta}_k)$, the corresponding power allocation and driving velocity of the kth vehicle can be respectively expressed by

$$p_k(\eta) = \frac{BN_k}{\delta_k\theta_k}\left[\frac{cm-\eta}{\Theta_k}W_0\left(\frac{\Theta_k 2^{q_k/B}}{cm-\eta}\mathrm{e}^{\frac{\Theta_k-\Upsilon_k}{cm-\eta}}\right)-1\right], \tag{25}$$

and

$$v_k(\eta) = \frac{B}{m}\log_2\left[\frac{cm-\eta}{\Theta_k}W_0\left(\frac{\Theta_k 2^{q_k/B}}{cm-\eta}\mathrm{e}^{\frac{\Theta_k-\Upsilon_k}{cm-\eta}}\right)\right]-\frac{q_k}{m}, \tag{26}$$

where

$$\Theta_k = \frac{\varsigma m N_k \ln 2}{\varphi M \delta_k \theta_k}, \text{ and} \tag{27}$$

$$\Upsilon_k = \frac{m\ln 2}{B}\left(\frac{a_0+Mb_0}{K}+a_1+Mb_1+cq_k\right). \tag{28}$$

Proof. Please see Appendix B. □

Based on the convexity of the vehicle PVR given in *Theorem 2*, we have the following corollary.

Corollary 1: When $\sum_{k=1}^{K} p_k(\tilde{\eta}) > p_{\mathrm{M}}$, all the vehicles should have the same PVR in order to minimize the maximum vehicle PVR, i.e.,

$$\eta_1(p_1) = \eta_2(p_2) = \cdots = \eta_K(p_K). \tag{29}$$

Proof. Please see Appendix C. □

Based on *Theorems 1–2*, *Corollary 1* and taking into account the total transmit power constraint in (12), we next discuss the optimal power allocation formulated in Algorithm 1 for minimizing the maximum PVR of all vehicles. As illustrated in Fig. 2 (where three vehicles are considered in our example), three cases exist in Algorithm 1 in terms of the total transmit power constraint value, namely a NRPC, strict power constraint (SPC) and medium power constraint (MPC).

- Case 1 (NRPC): All the vehicles can achieve their optimal PVRs, i.e.,

$$\sum\nolimits_{k=1}^{K}\tilde{p}_k < p_{\mathrm{M}}. \tag{30}$$

Therefore, the optimal power allocation can be expressed as $p_k^* = \tilde{p}_k\,(k\in\mathcal{K})$, which can be seen in lines 1,19-21 of Algorithm 1, and the min-max vehicle PVR is $\eta^* = \tilde{\eta} = \max_{k\in\mathcal{K}}\{\tilde{\eta}_k\}$.

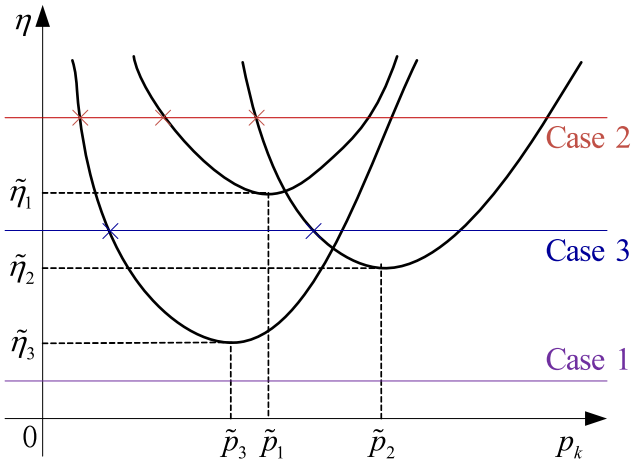

Fig. 2. Illustration of the power allocation for three cases.

- Case 2 (SPC): Not all the vehicles could achieve their optimal PVRs, i.e.,

$$\sum\nolimits_{k=1}^{K}\tilde{p}_k > p_{\mathrm{M}}, \text{ and } \sum\nolimits_{k=1}^{K} p_k(\tilde{\eta}) > p_{\mathrm{M}}. \tag{31}$$

Based on *Corollary 1*, all the vehicles should have the same PVR, i.e., $\eta^* > \tilde{\eta} = \max_{k\in\mathcal{K}}\{\tilde{\eta}_k\}$, therefore the min-max PVR and the power allocation can be obtained using the classic bi-section search of Algorithm 2 based on *Theorem 2*, which can be seen in lines 1-4, 15-18. The lower bound of η_k is given by $\eta_{\mathrm{L}} = \max_{k\in\mathcal{K}}\{\tilde{\eta}_k\} < \eta^*$, while the upper bound can be set as $\eta_{\mathrm{U}} = \max_{k\in\mathcal{K}}\{\eta_k(p_{k\mathrm{m}} + (p_{\mathrm{M}}-p_{\mathrm{m}})/K)\} > \eta^*$ due to the convexity of $\eta_k(p_k)$ $(k\in\mathcal{K})$, which is proved in *Theorem 2*.

- Case 3 (MPC): Part of the vehicles could achieve their optimal PVRs, i.e.,

$$\begin{aligned}&\sum\nolimits_{k=1}^{K}\tilde{p}_k > p_{\mathrm{M}}, \text{ and } \exists\ i\in\mathcal{K} \text{ s.t.}\\ &\sum\nolimits_{k=1}^{K}\left[p_k(\tilde{\eta}_i)\,I(\tilde{\eta}_k\le\tilde{\eta}_i)+\tilde{p}_k I(\tilde{\eta}_k>\tilde{\eta}_i)\right] < p_{\mathrm{M}},\end{aligned} \tag{32}$$

where $I(\cdot)\in\{0,1\}$ represents the indicative function. In Case 3, the optimal PVR is the same as that of Case 1, i.e., $\eta^* = \tilde{\eta} = \max_{k\in\mathcal{K}}\{\tilde{\eta}_k\}$. Based on *Corollary 1*, the vehicles that fail to achieve their optimal PVRs should have the same minimum PVR, which can be obtained by the bi-section search in a countable number of ranges $\left[\tilde{\eta}_{(k-1)}, \tilde{\eta}_{(k)}\right]$ $(k\in\mathcal{K})$, where $\tilde{\eta}_{(k)}$ $(k\in\mathcal{K})$ are sorted in increasing order. The corresponding pseudocodes are listed in lines 4-14 of Algorithm 1.

The computation complexity of the proposed Algorithm 1 is mainly determined by that of the bi-section search of Algorithm 2. Upon denoting the number of iterations by T and noting that $[\max_{k\in\mathcal{K}}\{\eta_k(p_{k\mathrm{m}}+(p_{\mathrm{M}}-p_{\mathrm{m}})/K)\}-cm]/2^T \le \varepsilon$ is a sufficient condition for Algorithm 2 to stop based on the termination condition $\eta_{\mathrm{U}}-\eta_{\mathrm{L}} \le \varepsilon$, the complexity of

Algorithm 1 Optimal Power Allocation for Vehicle PVR

Input: Initialize $p_k = \tilde{p}_k\,(k \in \mathcal{K})$ and error tolerance $\varepsilon > 0$.
Output: Power allocation $p_k^*\ (k \in \mathcal{K})$.

if $\sum_{k=1}^{K} p_k > p_{\mathrm{M}}$ **then**
  Let $\eta = \max\limits_{k\in\mathcal{K}} \{\tilde{\eta}_k\}$;
  Obtain $p_k\,(\eta)\ (k \in \mathcal{K})$ based on (25);
  if $\sum_{k=1}^{K} p_k < p_{\mathrm{M}}$ **then**
    Sort $\tilde{\eta}_k$ into $\tilde{\eta}_{(k)}\,(k \in \mathcal{K})$ by increasing order.
    Initialize $k = 0$;
    while $\sum_{i=1}^{k} p_{(i)} + \sum_{i=k+1}^{K} \tilde{p}_{(i)} > p_{\mathrm{M}}$ **do**
      $k = k + 1$;
      $\eta = \tilde{\eta}_{(k+1)}$;
      Obtain $p_{(i)}(\eta)\,(i = 1, 2, \cdots, k)$ based on (25);
    end while
    Let $\eta_{\mathrm{L}}{=}\eta_{(k)}$, $\eta_{\mathrm{U}}{=}\eta_{(k+1)}$, $p_{\mathrm{M}}{=}p_{\mathrm{M}}{-}\sum_{i=k+1}^{K} p_{(i)}$;
    Using Algorithm 2 to obtain $p_{(i)}^*\ (i = 1, 2, \cdots, k)$;
    Let $p_{(i)}^* = \tilde{p}_{(i)}\,(i = k+1, \cdots, K)$.
  else
    Let $\eta_{\mathrm{L}}{=}\max\limits_{k\in\mathcal{K}} \{\tilde{\eta}_k\}, \eta_{\mathrm{U}}{=}\max\limits_{k\in\mathcal{K}} \left\{\eta_k \left(p_{k\mathrm{m}}{+}\frac{p_{\mathrm{M}}-p_{\mathrm{m}}}{K}\right)\right\}$;
    Using Algorithm 2 to obtain $p_k^*\,(k \in \mathcal{K})$.
  end if
else
  $p_k^* = p_k\,(k \in \mathcal{K})$.
end if

Algorithm 2 Bi-Section Power Allocation

Input: Lower bound η_{L}, upper bound η_{U}, constraint power p_{M}, and error tolerance $\varepsilon > 0$.
Output: Power allocation p_k.

while $\eta_{\mathrm{U}} - \eta_{\mathrm{L}} > \varepsilon$ **do**
  $\eta = (\eta_{\mathrm{L}} + \eta_{\mathrm{U}})/2$;
  Calculate $p_k(\eta)\,(k \in \mathcal{K})$ based on (25);
  if $\sum_{k=1}^{K} p_k < p_{\mathrm{M}}$ **then**
    $\eta_{\mathrm{U}} = \eta$;
  else
    $\eta_{\mathrm{L}} = \eta$;
  end if
end while

Algorithm 1 can be formulated as being on the order of

$$T \sim \mathcal{O}\left(\log_2\left[\frac{\max_{k\in\mathcal{K}}\{\eta_k\,(p_{k\mathrm{m}}{+}(p_{\mathrm{M}}{-}p_{\mathrm{m}})/K)\}-cm}{\varepsilon}\right]\right). \tag{33}$$

C. Asymptotic Analysis under Strict Transmit Power Constraint

By bearing in mind that the transmit power constraint is low enough and the number of antennas becomes high, we formulate asymptotic expressions for both the velocity and power allocation in *Corollary 2*, which could simplify the calculations of velocity and power allocation.

Corollary 2: When the transmit power constraint p_{M} approximates to p_{m} at the BS, the velocity and power allocation of the kth vehicle respectively tend to

$$p_k\,(\eta) = \frac{BN_k}{\delta_k\theta_k}\left[\exp\left(\frac{\Upsilon_k}{\eta - cm} + \frac{q_k \ln 2}{B}\right) - 1\right], \tag{34}$$

$$v_k\,(\eta) = \frac{B\Upsilon_k \log_2 \mathrm{e}}{m\,(\eta - cm)}, M \gg 1, k \in \mathcal{K}. \tag{35}$$

Proof. Please see Appendix D. □

IV. Optimization of the System PVR

This section will first derive the general power allocation solution of the problems (15)–(19), based on which an iterative power allocation algorithm is proposed in order to achieve the minimum system PVR. Furthermore, the asymptotic system PVR is also discussed under a non-restrictive transmit power constraint.

A. Power Allocation for System PVR

Theorem 3: In order to achieve the minimum system PVR η_{S}^*, the optimal power allocation and driving velocity of the kth vehicle can be respectively expressed as:

$$p_k^*\,(\eta_{\mathrm{S}}^*, \mu) = \left[\frac{(\eta_{\mathrm{S}}^* - cm)\,B}{(\varsigma/\varphi M + \mu)\,m \ln 2} - \frac{BN_k}{\delta_k\theta_k}\right]_{p_{k\mathrm{m}}}^{p_{k\mathrm{M}}}, \tag{36}$$

and

$$v_k^*\,(\eta_{\mathrm{S}}^*, \mu) = \left[\frac{B}{m}\log_2\left(\frac{\delta_k\theta_k\,(\eta_{\mathrm{S}}^* - cm)}{(\varsigma/\varphi M + \mu)\,mN_k \ln 2}\right) - \frac{q_k}{m}\right]_0^{v_{\mathrm{M}}}, \tag{37}$$

where the Lagrange multiplier is either $\mu = 0$ or satisfies $\sum_{k=1}^{K} p_k^*\,(\eta_{\mathrm{S}}^*, \mu) = p_{\mathrm{M}}$ and $p_{k\mathrm{M}} = \frac{BN_k}{\delta_k\theta_k}\left(2^{\frac{mv_{\mathrm{M}}+q_k}{B}} - 1\right)$ $(k \in \mathcal{K})$. Moreover, the minimum system PVR may be obtained by bi-section search.

Proof. Please see Appendix E. □

B. Algorithm Design for System PVR

Based on *Theorem 3* and (81), we can achieve the minimum system PVR by using the classic bi-section search in Algorithm 3, where the initial values of the lower bound $\eta_{\mathrm{S}}^{\mathrm{L}}$ and upper bound $\eta_{\mathrm{S}}^{\mathrm{U}}$ constitute the range $\eta_{\mathrm{S}}^* \in \left[\eta_{\mathrm{S}}^{\mathrm{L}}, \eta_{\mathrm{S}}^{\mathrm{U}}\right]$. Based on (76), $\eta_{\mathrm{S}}^* \geq cm$ and therefore we set $\eta_{\mathrm{S}}^{\mathrm{L}} = cm$; on the other hand, $\eta_{\mathrm{S}}(\mathbf{p})$ is a quasi-convex function, hence $\mathbf{p} \succeq \mathbf{0}$ can make $\eta_{\mathrm{S}}(\mathbf{p}) \geq \eta_{\mathrm{S}}^*$ valid and therefore we set $\eta_{\mathrm{S}}^{\mathrm{U}} = \eta_{\mathrm{S}}(\mathbf{p}_{\mathrm{m}} + \mathbf{1}\,(p_{\mathrm{M}} - p_{\mathrm{m}})/K)$.

On the other hand, when $\mu \neq 0$, i.e., $\mu > 0$, we can find μ by exploiting $\sum_{k=1}^{K} p_k\,(\eta) - p_{\mathrm{M}} = 0$ based on bi-section search as seen in lines 8-18 in Algorithm 3. According to (87), the initial values of the lower bound μ_{L} and of the upper bound μ_{U} should satisfy $\mu_{\mathrm{L}} < \mu < \mu_{\mathrm{U}}$. Due to $\mu > 0$, we can set $\mu_{\mathrm{L}} = 0$; and the maximum power allocation among the vehicles should meet $\max\{p_k\,(\eta_{\mathrm{S}}, \mu)\} > 0$, i.e.,

$$\mu < \mu_{\mathrm{U}} = \left[\max_{k\in\mathcal{K}}\left\{\frac{\delta_k\theta_k}{N_k 2^{q_k/B}}\right\}\frac{\eta_{\mathrm{S}} - cm}{m \ln 2} - \frac{\varsigma}{\varphi M}\right]^+. \tag{38}$$

Moreover, for $\mu > 0$, if we have $p_{k\mathrm{m}} < p_k(\eta_{\mathrm{S}}, \mu) < p_{k\mathrm{M}}$ $(k \in \mathcal{K})$ in (36), i.e.,

$$\frac{BN_k}{\delta_k\theta_k}2^{\frac{q_k}{B}} < \frac{(\eta_{\mathrm{S}} - cm)B}{(\varsigma/\varphi M + \mu)m\ln 2} < \frac{BN_k}{\delta_k\theta_k}2^{\frac{mv_{\mathrm{M}}+q_k}{B}}, \quad (39)$$

which can be transformed into $\bar{\mu}_{\mathrm{L}} < \mu < \bar{\mu}_{\mathrm{U}}$ with

$$\bar{\mu}_{\mathrm{L}} = \left[\max_{k\in\mathcal{K}}\left\{\frac{\delta_k\theta_k}{N_k 2^{(mv_{\mathrm{M}}+q_k)/B}}\right\}\frac{\eta_{\mathrm{S}} - cm}{m\ln 2} - \frac{\varsigma}{\varphi M}\right]^+, \quad (40)$$

$$\bar{\mu}_{\mathrm{U}} = \left[\min_{k\in\mathcal{K}}\left\{\frac{\delta_k\theta_k}{N_k 2^{q_k/B}}\right\}\frac{\eta_{\mathrm{S}} - cm}{m\ln 2} - \frac{\varsigma}{\varphi M}\right]^+. \quad (41)$$

Then the following equation holds,

$$\sum_{k=1}^{K} p_k(\eta_{\mathrm{S}}, \mu) = \frac{K(\eta_{\mathrm{S}} - cm)B}{(\varsigma/\varphi M + \mu)m\ln 2} - \sum_{k=1}^{K}\frac{N_k B}{\delta_k\theta_k} = p_{\mathrm{M}}, \quad (42)$$

which results in

$$\mu = \frac{K(\eta_{\mathrm{S}} - cm)B}{\left(p_{\mathrm{M}} + \sum_{k=1}^{K}\frac{N_k B}{\delta_k\theta_k}\right)m\ln 2} - \frac{\varsigma}{\varphi M}. \quad (43)$$

Therefore, the bi-section search in lines 8-18 can be replaced by lines 5-6 of Algorithm 3, which can significantly reduce the algorithmic complexity.

Algorithm 3 contains a pair of nested loops, therefore its computational complexity is dominated by that of its inner and outer loops. The complexities of both the inner and outer loops are the same as that of Algorithm 1. Hence, we can express the total complexity order of Algorithm 3 as $\mathcal{O}\left(\log_2\left[\frac{\eta_{\mathrm{S}}(\mathbf{p}_{\mathrm{m}} + \mathbf{1}(p_{\mathrm{M}} - p_{\mathrm{m}})/K) - cm}{\varepsilon}\right] \times \log_2\left(\frac{\mu_{\mathrm{U}}}{\omega}\right)\right)$. However, the inner loop may not be necessary when $\bar{\mu}_{\mathrm{L}} < \mu < \bar{\mu}_{\mathrm{U}}$, hence the total complexity may be significantly simplified.

C. Asymptotic Analysis under Non-Restrictive Power Constraint

When the total transmit power constraint is high enough for the system PVR to ignore the constraint (18) for the problems in (15)–(19), the optimal power allocation can be calculated by setting $\mu = 0$ in *Theorem 3*. Then the achievable system PVR can be obtained by Algorithm 3 upon bypassing lines 4-21. Alternatively, we can also obtain the minimum system PVR by the following theorem.

Theorem 4: When the transmit power constraint is high enough to become non-restrictive, the optimal power allocation minimizing the system PVR is the same as that minimizing the maximum vehicle PVR. Explicitly, it becomes identical to *Theorem 1*. Then, the minimum system PVR can be expressed as

$$\tilde{\eta}_{\mathrm{s}} = \frac{\sum_{k=1}^{K} p_{\mathrm{T}k}(\tilde{p}_k)}{\sum_{k=1}^{K} v_k(\tilde{p}_k)}. \quad (44)$$

Proof. Please see Appendix F. □

V. Simulation Results and Analysis

This section first defines the parameter setup of our vehicular system. Then, the vehicle PVR and system PVR are respectively evaluated under different power allocation schemes. Finally, the vehicle PVR and system PVR are compared under the optimal power allocation schemes for minimizing the maximum vehicle PVR and system PVR, respectively.

Algorithm 3 Optimal Power Allocation for System PVR

Input: Lower bound η_{L}, upper bound η_{U}, constraint power p_{M}, and error tolerance $\varepsilon > 0$.
Output: Power allocation p_k.

1: **while** $\eta_{\mathrm{S}}^{\mathrm{U}} - \eta_{\mathrm{S}}^{\mathrm{L}} > \varepsilon$ **do**
2: $\eta_{\mathrm{S}} = \left(\eta_{\mathrm{S}}^{\mathrm{L}} + \eta_{\mathrm{S}}^{\mathrm{U}}\right)/2$;
3: Calculate $p_k(\eta_{\mathrm{S}}, 0)$ based on (36);
4: **if** $\sum_{k=1}^{K} p_k > p_{\mathrm{M}}$ **then**
5: **if** $\bar{\mu}_{\mathrm{L}} < \mu < \bar{\mu}_{\mathrm{U}}$ **then**
6: Calculate μ according to (43).
7: **else**
8: Initialize μ_{L} and μ_{U} with zero and (38);
9: Initialize the error tolerance $\omega > 0$.
10: **while** $\mu_{\mathrm{U}} - \mu_{\mathrm{L}} > \omega$ **do**
11: $\mu = (\mu_{\mathrm{L}} + \mu_{\mathrm{U}})/2$
12: Calculate $p_k(\eta_{\mathrm{S}}, \mu)$ based on (36);
13: **if** $\sum_{k=1}^{K} p_k > p_{\mathrm{M}}$ **then**
14: $\mu_{\mathrm{L}} = \mu$;
15: **else**
16: $\mu_{\mathrm{U}} = \mu$;
17: **end if**
18: **end while**
19: **end if**
20: Calculate $p_k(\eta_{\mathrm{S}}, \mu)$ based on (36);
21: **end if**
22: **if** $f(\mathbf{p}, \eta_{\mathrm{S}}) > 0$ **then**
23: $\eta_{\mathrm{S}}^{\mathrm{L}} = \eta_{\mathrm{S}}$;
24: **else**
25: $\eta_{\mathrm{S}}^{\mathrm{U}} = \eta_{\mathrm{S}}$;
26: **end if**
27: **end while**
28: Calculate $p_k^*(\eta_{\mathrm{S}}, \mu)$ based on (36);

A. Simulation Setup

In the simulations, the default parameters are given as follows. The number of antennas at the BS is $M = 128$, the number of vehicles is $K = 10$, the system bandwidth is $B = 200$ kHz, and the total transmit power is $p_{\mathrm{M}} = 24 + 10\log_{10}M$ dBm. As shown in Fig. 1, All vehicles are uniformly distributed on two lanes with the length $L = 100$ m, the width of each lane is $W = 5$ m, and the vertical distance between the BS and the nearest lane is $H = 15$ m. The maximum velocity of each vehicle is $v_{\mathrm{M}} = 35$ m/s, the position-related information requirement of each vehicle per meter is $m = 2.5 \times 10^5$ bit/m, and the information overhead $q_k = 10^4$ bit/s $(k \in \mathcal{K})$ [17], [34], [35], [47].

The large-scale fading coefficients are $\delta_k = 10^{-3}d_k^{-4}\zeta_k$ $(k \in \mathcal{K})$, where d_k represents the distance between the BS and the kth vehicle, and ζ_k denotes the log-normal shadow fading obeying $10\log_{10}\zeta_k \sim \mathbb{N}\left(0, \sigma_{\mathrm{SF}}^2\right)$ with $\sigma_{\mathrm{SF}} = 8$ dB [41], [42]. The noise power spectral density is assumed to be $N_k = -174$ dBm/Hz $(k \in \mathcal{K})$ [51].

At the BS, the power efficiency of PAs is $\varphi = 0.35$, the PAPR is $\varsigma = 1.2705$, the coefficients of the circuit power dissipation model are $[a_0, a_1] = [20, 0.1]$ W, $[b_0, b_1] = \left[1, 2.6 \times 10^{-8}\right]$ W, and c=1.15×10^{-9} W [44], [45].

In the following figures, all results are the average of 10^6 realizations of vehicle distribution on the lanes. "PCSI" and "ECSI" represent the results of perfect CSI ($\theta_k = 1, k \in \mathcal{K}$) and estimated CSI ($\theta_k = 0.6, k \in \mathcal{K}$), respectively.

B. Vehicle PVR Results

With one-time realization of the channel under $p_{\rm M} = 10\log_{10}M$ dBm, Fig. 3 illustrates the vehicle PVR of Case 2 versus the number of iterations in Algorithm 2 under $\varepsilon = 10^{-6}$. In Fig. 3, $\eta_{\rm L}$, $\eta_{\rm U}$ and η represent the lower bound, upper bound and the actually obtained PVR of each iteration, respectively. Upon increasing the number of iterations, the lower bound increases, the upper bound decreases, and they rapidly converge to a constant, which verifies the convergence of Case 2 in Algorithm 2 under both perfect and estimated CSI. Moreover, the convergence behavior of Algorithm 2 under Case 3 is similar to that under Case 2. Hence, the convergence of Algorithm 1 is verified.

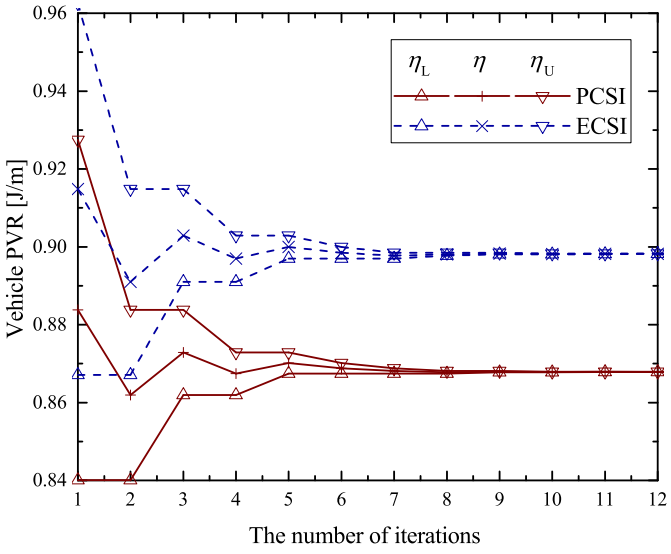

Fig. 3. Vehicle PVR versus the number of iterations in Algorithm 2.

Fig. 4 shows the maximum PVR, PVR mean and minimum PVR among all vehicles versus the transmit power constraint $p_{\rm M}$ at the BS under both perfect and estimated CSI. When the transmit power constraint is low (below 25 dBm), the maximum PVR is the same to the minimum PVR, i.e., the PVRs of all vehicles are the same, which verifies Algorithm 1 under Case 2. By contrast when the transmit power constraint is high enough (higher than 35 dBm), the maximum PVR, PVR mean and minimum PVR converge to their un-restricted values, respectively, i.e., the PVR of each vehicle converges to its minimum value, which verifies Algorithm 1 under Case 1. When the transmit power constraint is mediocre, the maximum PVR is the same as that under Case 1. However, the minimum PVR and PVR mean are higher than those under Case 1, i.e., part of the vehicles can achieve their minimum PVRs, which verifies Algorithm 1 under Case 3. Hence, the results seen in Fig. 4 are consistent with the analysis of Algorithm 1. Moreover, the maximum PVR, PVR mean and minimum PVR under perfect CSI are lower than those under estimated CSI. This trend is not unexpected because some extra power is required in the presence of imperfect CSI estimates.

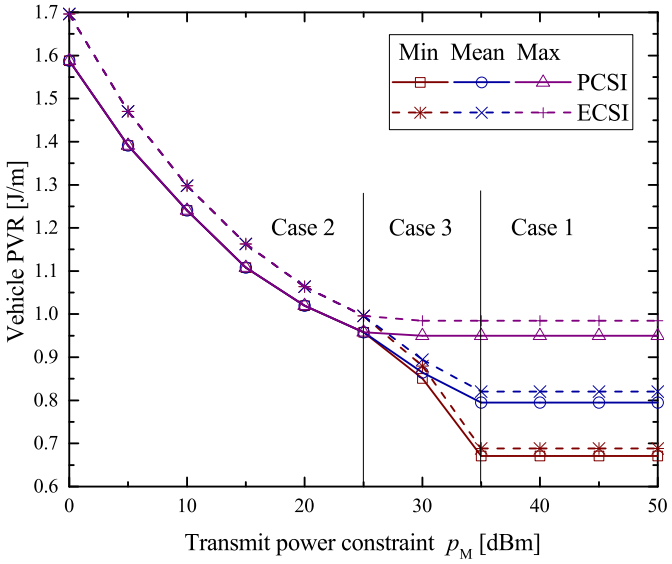

Fig. 4. Vehicle PVR versus the transmit power constraint under the optimal power allocation scheme.

Fig. 5 illustrates the maximum PVR among all vehicles for the different schemes versus the transmit power constraint $p_{\rm M}$ at the BS under both perfect and estimated CSI. The maximum PVRs of NRPC or no transmit power constraint are calculated by (24). The maximum PVRs under the optimal power allocation (OPA) are simulated by Algorithm 1. By contrast, the maximum PVRs under equal power allocation (EPA) are calculated by (64) using $p_k = p_{\rm M}/K$ $(k \in \mathcal{K})$. Observe in Fig. 5 that upon increasing the transmit power constraint $p_{\rm M}$, the maximum PVR under EPA first decreases and then increases. The maximum PVR of NRPC remains constant under perfect CSI or estimated CSI. Furthermore, the maximum PVR under the proposed OPA scheme first decreases and then becomes constant at the maximum PVR of the NRPC scenario. The maximum PVR under the proposed OPA scheme is lower than that of EPA. Moreover, the maximum PVRs of the three schemes evaluated under perfect CSI are lower than those under the estimated CSI; and the maximum PVRs of $K = 30$ are more attractive than those of $K = 10$, because the second term of the power consumption in (7) reduced upon increasing the number of vehicles.

In parallel to the OPA scheme of Fig. 4, Fig. 6 depicts the maximum velocity, velocity mean and minimum velocity under Algorithm 1 versus the transmit power constraint. We also have the similar conclusions to those of vehicle PVR in Fig. 4. However, different from vehicle PVR, the reason for that the maximum velocity, velocity mean and minimum

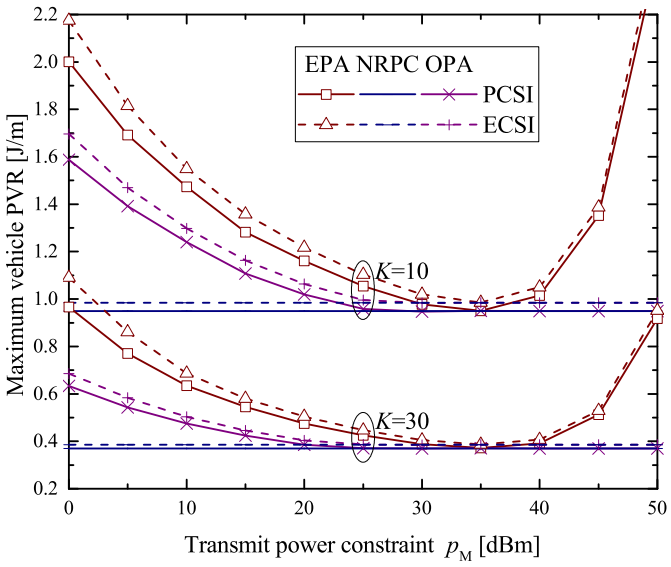

Fig. 5. Maximum vehicle PVR versus the transmit power constraint.

velocity have the same value in the region of low transmit power constraint, has been proved in *Corollary 2*.

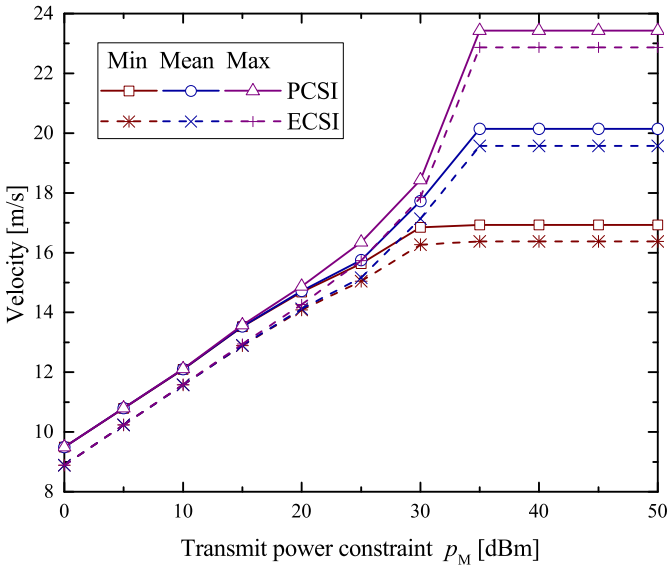

Fig. 6. Velocity versus the transmit power constraint under the optimal power allocation for vehicle PVR.

C. System PVR Results

Figs. 7 and 8 illustrate the system PVR and velocity versus the transmit power constraint, respectively. The results of OPA scheme are calculated by Algorithm 3, the results under NRPC are given by *Theorem 4* or *Theorem 1*, and the results of EPA scheme are calculated by (76) and (63) with $p_k = p_{\mathrm{M}}/K$ $(k \in \mathcal{K})$. From Fig. 7, the system PVR under NRPC outperforms that of EPA scheme in the regions of both low and high transmit power. However, in the region of mediocre transmit power, they have the similar performance because the term $N_k B/\delta_k \theta_k$ is too small in (36) and the power allocation under NRPC can be approximated by $p_k^* = \left(\eta_{\mathrm{S}}^* - cm\right) B/[(\varsigma/\varphi M + \mu)\, m \ln 2]$, i.e., the EPA scheme. The system PVRs in the region of high transmit power become constants or have no relationship to the transmit power constraint, which have been proved by *Theorem 4*. The system PVRs of $K = 30$ are more attractive than those of $K = 10$ under the three power allocation schemes considered, because the circuit power consumption in (7) is divided among more vehicles. Fig. 8 indicates that the maximum velocity is larger than the velocity mean and the minimum velocity; with the increasing transmit power constraint, they first increase and finally keep constants, which also have been proved in *Theorem 4*. Moreover, the system PVRs and vehicle velocities under perfect CSI perform better than those under estimated CSI due to the effect of channel estimation error.

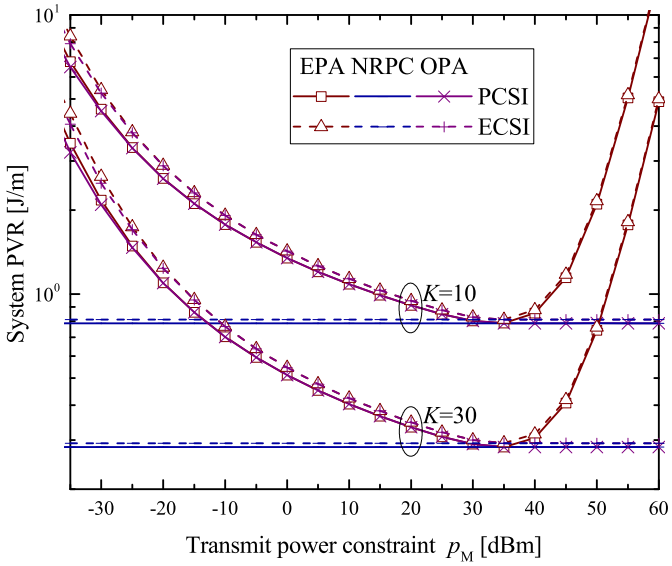

Fig. 7. System PVR versus the transmit power constraint.

D. Comparison of Two Optimal Power Allocation Schemes

Figs. 9 and 10 illustrate the vehicle PVR and system PVR versus the transmit power constraint under our pair of OPA schemes minimizing either the maximum vehicle PVR or the system PVR, respectively. As seen in Fig. 9, the OPA scheme minimizing the vehicle PVR has better fairness among all vehicles than that of the system PVR optimization. By contrast, in Fig. 10, the OPA scheme minimizing the system PVR outperforms the vehicle-based PVR regime. However, in the region of high transmit power, they have a similar PVR, which was formally shown in *Theorem 4*. Moreover, the PVRs under the pair of our OPA schemes minimizing either the maximum vehicle PVR or the system PVR versus the channel estimation accuracy θ are depicted in Fig. 11. Both the optimal vehicle PVR and system PVR are improved upon increasing the estimation accuracy, because the channel gains are gradually improved; the system PVR is lower than

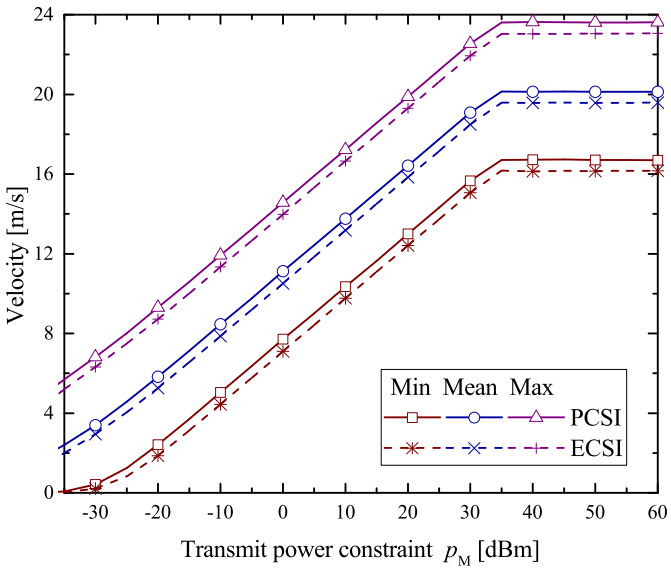

Fig. 8. Velocity versus the transmit power constraint under the optimal power allocation for system PVR.

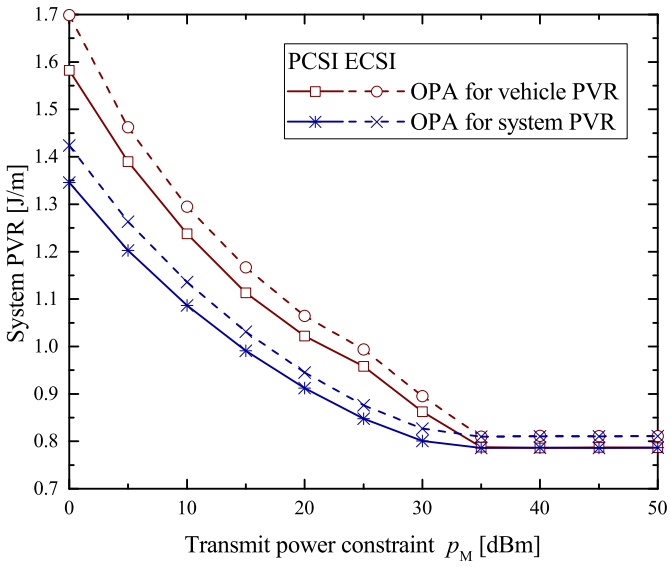

Fig. 10. System PVR versus the transmit power constraint.

the vehicle PVR, albeit the reduced system PVR is attained at the cost of reduced fairness among vehicles, as observed in Fig. 9.

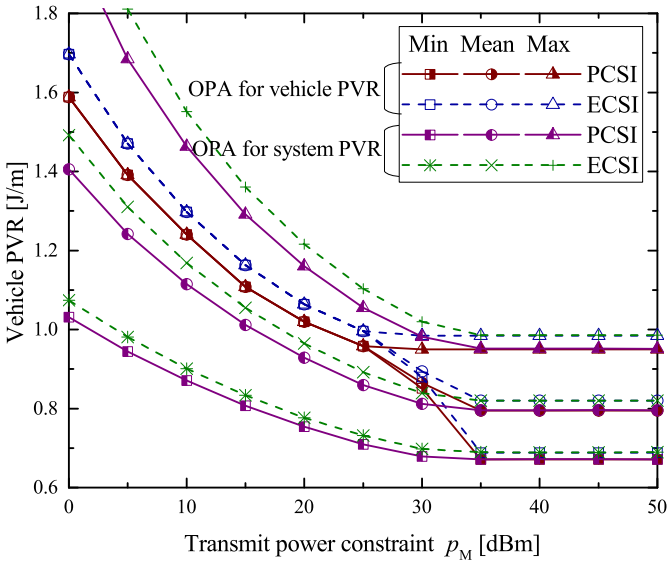

Fig. 9. Maximum vehicle PVR versus the transmit power constraint.

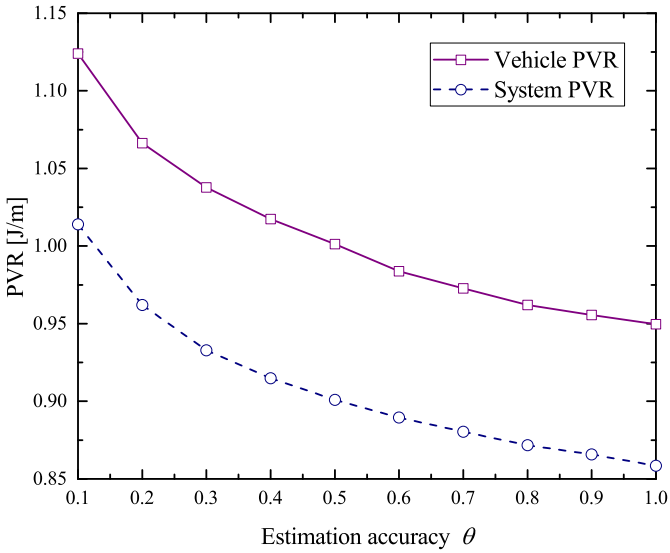

Fig. 11. PVR versus the channel estimation accuracy.

VI. Conclusions

In order to jointly characterize the communications resource consumption and the road-traffic efficiency, we studied the PVR of vehicular networks, which physically represents the energy requirement per unit driving distance of vehicles, which is of course proportional to the velocity. Considering the fairness among all vehicles, first the min-max problem of vehicle PVR was investigated and the optimal power allocation algorithm was proposed by taking into account different transmit power constraints. Then the PVR minimization problem was studied and an efficient power allocation algorithm was designed using the classic bi-section search. Moreover, the asymptotic PVR performance of both the individual vehicles and of the entire system was also analyzed in the regions of both low and high transmit powers. Our simulation results verified the efficiency of the proposed power allocation algorithms.

Appendix A
Proof of Theorem 1

When the number of antennas M is high at the BS, the asymptotic channel orthogonality and channel hardening effect

hold [36], [41], i.e.,

$$\frac{1}{M}\hat{\mathbf{h}}_k^{\mathrm{T}}\hat{\mathbf{h}}_i^* \to 0,\ k \neq i, M \to \infty, \tag{45}$$

$$\frac{1}{M}\hat{\mathbf{h}}_k^{\mathrm{T}}\mathbf{e}_i^* \to 0, \forall\ k, i \in \mathcal{K},\ M \to \infty, \tag{46}$$

$$\frac{1}{M}\hat{\mathbf{h}}_k^{\mathrm{T}}\hat{\mathbf{h}}_k^* \to 1,\ \forall\ k \in \mathcal{K}, M \to \infty. \tag{47}$$

Based on this and upon substituting (2) into (4), the SINR of the kth vehicle can be simplified to

$$\begin{aligned}\gamma_k(\mathbf{p}) &= \frac{p_k\left\|\hat{\mathbf{h}}_k\right\|^2}{\sum\limits_{i=1,\neq k}^{K} p_i\frac{\left|\hat{\mathbf{h}}_k^{\mathrm{T}}\hat{\mathbf{h}}_i^*\right|^2}{\left\|\hat{\mathbf{h}}_i\right\|^2} + \frac{1-\theta_k}{\theta_k}\sum\limits_{i=1}^{K} p_i\frac{\left|\mathbf{e}_k^{\mathrm{T}}\hat{\mathbf{h}}_i^*\right|^2}{\left\|\hat{\mathbf{h}}_i\right\|^2} + \frac{MN_kB}{\delta_k\theta_k}} \\ &\to \frac{p_k\delta_k\theta_k}{N_kB}, M \to \infty,\end{aligned} \tag{48}$$

and the transmission rate in (5) can be rewritten as

$$r_k(p_k) = B\log_2\left(1 + \frac{p_k\delta_k\theta_k}{N_kB}\right). \tag{49}$$

Substituting (49) into (7), the numerator $p_{\mathrm{T}k}$ of the objective function (9) is a monotonically increasing function with respect to p_k; on the other hand, the objective function (9) is a monotonically decreasing function with respect to v_k. Therefore, the equality of constraint (10) should hold in order to minimize the vehicle PVR, i.e.,

$$r_k(p_k) = mv_k + q_k. \tag{50}$$

Therefore, when the information overhead $q_k = 0$ ($k \in \mathcal{K}$), the transmit rate is proportional to the driving velocity for each vehicle, and the proposed PVR becomes similar to the concept of EE [29]–[32].

Substituting (50) into (49) results in

$$p_k(v_k) = \frac{N_kB}{\delta_k\theta_k}\left\{\exp\left[\frac{\ln 2}{B}(mv_k + q_k)\right] - 1\right\}. \tag{51}$$

Then the objective function in (8) can be rewritten as

$$\eta_k(v_k) = \frac{\varsigma p_k(v_k)}{\varphi M v_k} + \frac{1}{v_k}\left(\frac{a_0 + Mb_0}{K} + a_1 + Mb_1 + cq_k\right) + cm. \tag{52}$$

When we dispense with the total transmit power constraint in (12), the problems formulated in (9)–(13) can be transformed into

$$\min_{v_k}\max_{k}\{\eta_k(v_k)\} \tag{53}$$

$$\text{s.t. } 0 \leq v_k \leq v_{\mathrm{M}}, k \in \mathcal{K}. \tag{54}$$

Since the PVRs $\eta_k(v_k)$ ($k \in \mathcal{K}$) of all vehicles are independent of each other, we have

$$\min_{v_k}\max_{k}\{\eta_k(v_k)\} = \max_{k}\min_{v_k}\{\eta_k(v_k)\}. \tag{55}$$

Therefore, the problems in (53)–(54) can be further simplified to K independent problems, yielding:

$$\min_{v_k}\{\eta_k(v_k)\} \quad \text{s.t. } 0 \leq v_k \leq v_{\mathrm{M}}. \tag{56}$$

The Lagrange function of (56) can be written as

$$\begin{aligned}\mathcal{L}_k(v_k;\lambda_k) =& \frac{\varsigma p_k(v_k)}{\varphi M v_k} + \frac{1}{v_k}\left(\frac{a_0 + Mb_0}{K} + a_1 + Mb_1 + cq_k\right) \\ &+ cm + \lambda_k(v_k - v_{\mathrm{M}}), k \in \mathcal{K},\end{aligned} \tag{57}$$

where $\lambda_k \geq 0$ ($k \in \mathcal{K}$) is the Lagrange multiplier. Applying the Karush-Kuhn-Tucker (KKT) conditions [52], we have

$$\frac{\mathrm{d}\mathcal{L}_k(v_k,\lambda_k)}{\mathrm{d}v_k} = 0, \tag{58}$$

$$\lambda_k(v_k - v_{\mathrm{M}}) = 0. \tag{59}$$

Based on (58), we arrive at:

$$\begin{aligned}\frac{\mathrm{d}\mathcal{L}_k(v_k;\lambda_k)}{\mathrm{d}v_k} =& \frac{1}{v_k^2}\frac{\varsigma BN_k 2^{\frac{q_k}{B}}}{\varphi M\delta_k\theta_k}\left\{\left(\frac{mv_k\ln 2}{B} - 1\right)2^{\frac{mv_k}{B}} - \mathrm{e}\Psi_k\right\} \\ &+ \lambda_k = 0.\end{aligned} \tag{60}$$

When $\lambda_k = 0$, (60) can be transformed into

$$\left(\frac{mv_k\ln 2}{B} - 1\right)\exp\left(\frac{mv_k\ln 2}{B} - 1\right) = \Psi_k > -\mathrm{e}^{-1}. \tag{61}$$

Taking advantage of the first real branch of the Lambert function gives rise to

$$v_k = \frac{B}{m\ln 2}\left[W_0(\Psi_k) + 1\right] \triangleq \hat{v}_k > 0. \tag{62}$$

Furthermore, upon taking into account (59), we have (20), substituting (20) into (51) and (52), respectively, yields the optimal power allocation (21) and individual PVR (22) for the problem (56).

Appendix B
Proof of Theorem 2

Substituting (50) into (51) results in

$$v_k(p_k) = \frac{B}{m}\log_2\left(1 + \frac{p_k\delta_k\theta_k}{N_kB}\right) - \frac{q_k}{m}, \tag{63}$$

and taking (63) into (52) yields

$$\eta_k(p_k) = \frac{\Theta_k\frac{p_k\delta_k\theta_k}{BN_k} + \Upsilon_k}{\ln\left(1 + \frac{p_k\delta_k\theta_k}{BN_k}\right) - \frac{q_k\ln 2}{B}} + cm, \tag{64}$$

where Θ_k and Υ_k are given in (27) and (28), respectively.

The first and second order derivatives of $\eta_k(p_k)$ with respect to p_k can be respectively expressed as

$$\begin{aligned}\frac{\mathrm{d}\eta_k(p_k)}{\mathrm{d}p_k} =& \frac{\frac{\Theta_k\delta_k\theta_k}{BN_k}}{\ln\left(1 + \frac{p_k\delta_k\theta_k}{BN_k}\right) - \frac{q_k\ln 2}{B}} - \\ &\frac{\frac{\delta_k\theta_k}{BN_k}\left(\frac{\Theta_k p_k\delta_k\theta_k}{BN_k} + \Upsilon_k\right)}{\left(1 + \frac{p_k\delta_k\theta_k}{BN_k}\right)\left[\ln\left(1 + \frac{p_k\delta_k\theta_k}{BN_k}\right) - \frac{q_k\ln 2}{B}\right]^2},\end{aligned} \tag{65}$$

and

$$\frac{\mathrm{d}^2\eta_k\left(p_k\right)}{\mathrm{d}p_k^2}=\frac{\frac{\frac{p_k\delta_k\theta_k}{BN_k}+\frac{\Upsilon_k}{\Theta_k}}{\frac{p_k\delta_k\theta_k}{BN_k}+1}+\frac{2\left(\frac{p_k\delta_k\theta_k}{BN_k}+\frac{\Upsilon_k}{\Theta_k}\right)}{\left(1+\frac{p_k\delta_k\theta_k}{BN_k}\right)\left[\ln\left(1+\frac{p_k\delta_k\theta_k}{BN_k}\right)-\frac{q_k\ln 2}{B}\right]^2}-2}{\frac{\left(1+\frac{p_k\delta_k\theta_k}{BN_k}\right)\left[\ln\left(1+\frac{p_k\delta_k\theta_k}{BN_k}\right)-\frac{q_k\ln 2}{B}\right]^2}{\Theta_k\left(\frac{\delta_k\theta_k}{BN_k}\right)^2}}$$
$$>\frac{\Theta_k\left(\frac{\delta_k\theta_k}{BN_k}\right)^2\left(\frac{\frac{p_k\delta_k\theta_k}{BN_k}+\frac{\Upsilon_k}{\Theta_k}}{\frac{p_k\delta_k\theta_k}{BN_k}+1}-2\right)}{\left(1+\frac{p_k\delta_k\theta_k}{BN_k}\right)\left[\ln\left(1+\frac{p_k\delta_k\theta_k}{BN_k}\right)-\frac{q_k\ln 2}{B}\right]^2}. \quad (66)$$

When the number of antennas at the BS becomes high, we can arrive at:

$$\frac{\Upsilon_k}{\Theta_k}>2+\frac{p_k\delta_k\theta_k}{N_kB}, M\gg 1. \quad (67)$$

Upon substituting (27) and (28) into (67), the number of antennas M should satisfy

$$\left(\frac{b_0}{K}+b_1\right)M^2+\left(\frac{a_0}{K}+a_1+cq_k\right)M>\frac{\varsigma}{\varphi}\left(p_k+2\frac{BN_k}{\delta_k\theta_k}\right), \quad (68)$$

which is equivalent to

$$M>\frac{\sqrt{\left(\frac{a_0}{K}+a_1+cq_k\right)^2+\frac{\varsigma}{\varphi}\left(\frac{b_0}{K}+b_1\right)\left(p_k+\frac{2BN_k}{\delta_k\theta_k}\right)}}{2\left(\frac{b_0}{K}+b_1\right)}-\frac{\frac{a_0}{K}+a_1+cq_k}{2\left(\frac{b_0}{K}+b_1\right)}. \quad (69)$$

Therefore, substituting (67) into (66) yields $\mathrm{d}^2\eta_k\left(p_k\right)/\mathrm{d}p_k^2>0$ and the PVR function $\eta_k\left(p_k\right)$ is a convex function with respect to the power p_k allocated to the kth vehicle.

If the PVR value η is given, then we have

$$\eta_k\left(p_k\right)=\frac{\Theta_k\frac{p_k\delta_k\theta_k}{BN_k}+\Upsilon_k}{\ln\left(1+\frac{p_k\delta_k\theta_k}{BN_k}\right)-\frac{q_k\ln 2}{B}}+cm=\eta, \quad (70)$$

which can be transformed into

$$\frac{\Theta_k\frac{p_k\delta_k\theta_k}{BN_k}+\Upsilon_k}{\eta-cm}=\ln\left(1+\frac{p_k\delta_k\theta_k}{BN_k}\right)-\frac{q_k\ln 2}{B}. \quad (71)$$

Applying the exponential operation to both sides of (71) and carrying out some further manipulations yields:

$$\frac{\Theta_k\left(1+\frac{p_k\delta_k\theta_k}{BN_k}\right)}{cm-\eta}\mathrm{e}^{\frac{\Theta_k\left(1+\frac{p_k\delta_k\theta_k}{BN_k}\right)}{cm-\eta}}=\frac{\Theta_k 2^{\frac{q_k}{B}}}{cm-\eta}\mathrm{e}^{\frac{\Theta_k-\Upsilon_k}{cm-\eta}}. \quad (72)$$

By exploiting the Lambert function results in (25), and substituting (25) into (63) yields (26).

Appendix C
Proof of Corollary 1

Equation (29) is proved by the method of contradiction. Let us assume that the optimal solution $\bar{p}_k\ (k\in\mathcal{K})$ of the problems in (9)–(13) satisfies

$$\eta_j\left(\bar{p}_j\right)>\eta_k\left(\bar{p}_k\right)>\eta_i\left(\bar{p}_i\right), k\neq i,j. \quad (73)$$

Then by taking into account $\sum_{k=1}^{K}p_k\left(\tilde{\eta}\right)>p_{\mathrm{M}}$ and the convexity in *Theorem 2*, both $\eta_j\left(\cdot\right)$ and $\eta_i\left(\cdot\right)$ are monotonically decreasing functions when $p_k<\tilde{p}_k$ $(k\in\mathcal{K})$. Hence there should exist a specific $\Delta\in\left(0,\bar{p}_i-N_kB\left(2^{q_k/B}-1\right)/(\delta_k\theta_k)\right)$ satisfying that

$$\eta_j\left(\bar{p}_j\right)>\eta_j\left(\bar{p}_j+\Delta\right)=\eta_i\left(\bar{p}_i-\Delta\right)>\eta_i\left(\bar{p}_i\right). \quad (74)$$

Then, we can define the new power allocation $p_j=\bar{p}_j+\Delta$, $p_i=\bar{p}_i-\Delta$ and $p_k=\bar{p}_k\left(k\neq i,j\right)$. Given the defined $p_k\left(k\in\mathcal{K}\right)$, the maximum PVR among vehicles decreases, which contradicts to the min-max criterion. Therefore, all vehicles should have the same vehicle PVR.

Appendix D
Proof of Corollary 2

Based on (27), we have $\Theta_k\to 0\ (k\in\mathcal{K})$ when the number of antennas M becomes large; on the other hand, $cm-\eta\nrightarrow 0$ if the PVR η is far away from the lower bound cm, when the transmit power constraint p_{M} approximates to p_{m}. Therefore, we have $\Theta_k/(cm-\eta)\to 0\ (M\gg 1)$. By exploiting the property of the Lambert function that $W_0\left(x\right)\to 0$ when $x\to 0$, we arrive at:

$$W_0\left(\frac{\Theta_k 2^{\frac{q_k}{B}}}{cm-\eta}\mathrm{e}^{\frac{\Upsilon_k-\Theta_k}{\eta-cm}}\right)\to\frac{\Theta_k 2^{\frac{q_k}{B}}}{cm-\eta}\mathrm{e}^{\frac{\Upsilon_k-\Theta_k}{\eta-cm}}, M\gg 1. \quad (75)$$

Substituting (75) and $\Theta_k\to 0$ into (25) and (26) results in (34) and (35), respectively.

Appendix E
Proof of Theorem 3

Following the same lines in the proof of *Theorem 1*, we should have $mv_k=B\log_2\left(1+\frac{p_k\delta_k\theta_k}{N_kB}\right)-q_k\ (k\in\mathcal{K})$, therefore substituting (7) into (14) and introducing $\mathbf{q}=\left[q_1,q_2,\cdots,q_K\right]^{\mathrm{T}}$ result in

$$\eta_{\mathrm{S}}\left(\mathbf{p}\right)=\frac{\frac{\varsigma\mathbf{1}^{\mathrm{T}}\mathbf{p}}{\varphi M}+a_0+Mb_0+K\left(a_1+Mb_1\right)+c\mathbf{1}^{\mathrm{T}}\mathbf{q}}{\frac{B}{m}\sum_{k=1}^{K}\log_2\left(1+\frac{p_k\delta_k\theta_k}{N_kB}\right)-\frac{\mathbf{1}^{\mathrm{T}}\mathbf{q}}{m}}+cm. \quad (76)$$

The denominator and numerator of the system PVR given in (76) are convex and affine functions with respect to the power allocation vector $\mathbf{p}$, respectively. Therefore the set $\{\mathbf{p}|\eta_{\mathrm{S}}\left(\mathbf{p}\right)<\eta\}$ is convex and hence the objective function $\eta_{\mathrm{S}}\left(\mathbf{p}\right)$ is a quasi-convex function with respect to the power allocation vector $\mathbf{p}$. Based on [31], [52], [53], if the fractional objective function given in (76) is quasi-convex in conjunction with a convex denominator and affine numerator, the optimization problems in (15)–(19) are equivalent to

$$\min_{\mathbf{p}}\left\{f\left(\mathbf{p},\eta\right)\right\} \quad (77)$$

$$\text{s.t. } 0\leq v_k\leq v_{\mathrm{M}}, k\in\mathcal{K}, \quad (78)$$

$$\mathbf{1}^{\mathrm{T}}\mathbf{p}\leq p_{\mathrm{M}}, \quad (79)$$

where the new objective function is defined by

$$f(\mathbf{p},\eta)=\frac{\varsigma\mathbf{1}^{\mathrm{T}}\mathbf{p}}{\varphi M}+a_0+Mb_0+K(a_1+Mb_1)+\frac{\eta}{m}\mathbf{1}^{\mathrm{T}}\mathbf{q}-\frac{(\eta-cm)B}{m}\sum\nolimits_{k=1}^{K}\log_2\left(1+\frac{p_k\delta_k\theta_k}{N_kB}\right), \quad (80)$$

and the optimal system PVR, η_{S}^*, satisfies

$$f(\mathbf{p},\eta)\begin{cases}<0, & \eta>\eta_{\mathrm{S}}^*,\\ =0, & \eta=\eta_{\mathrm{S}}^*,\\ >0, & \eta<\eta_{\mathrm{S}}^*.\end{cases} \quad (81)$$

Therefore, if the new problems in (77)–(79) are solved, then the optimal system PVR, η_{S}^*, can be obtained by bi-section search in terms of (81).

Given the system PVR η, the Lagrange function of problems (77)–(79) can be written as

$$\mathcal{L}(\mathbf{p};\boldsymbol{\lambda},\mu)=f(\mathbf{p},\eta)+\boldsymbol{\lambda}^{\mathrm{T}}(\mathbf{v}-\mathbf{1}v_{\mathrm{M}})+\mu\left(\mathbf{1}^{\mathrm{T}}\mathbf{p}-p_{\mathrm{M}}\right), \quad (82)$$

where $\boldsymbol{\lambda}=[\lambda_1,\lambda_2,\cdots,\lambda_K]^{\mathrm{T}}\succeq 0$ and $\mu\geq 0$ are the non-negative Lagrange multipliers. Based on the KKT conditions [52], we have

$$\mathrm{d}\mathcal{L}(\mathbf{p};\boldsymbol{\lambda},\mu)/\mathrm{d}p_k=0, k\in\mathcal{K}, \quad (83)$$

$$\lambda_k(v_k-v_{\mathrm{M}})=0, k\in\mathcal{K}, \quad (84)$$

$$\mu\left(\mathbf{1}^{\mathrm{T}}\mathbf{p}-p_{\mathrm{M}}\right)=0. \quad (85)$$

According to the first KKT condition (83), we can obtain

$$\begin{aligned}\frac{\mathrm{d}\mathcal{L}(\mathbf{p};\boldsymbol{\lambda},\mu)}{\mathrm{d}p_k}&=\frac{\mathrm{d}f(\mathbf{p},\eta)}{\mathrm{d}p_k}+\lambda_k\frac{\mathrm{d}v_k}{\mathrm{d}p_k}+\mu\\&=\frac{\varsigma}{\varphi M}+\frac{B}{m\ln 2}\frac{(\lambda_k-\eta+cm)\delta_k\theta_k}{N_kB+p_k\delta_k\theta_k}+\mu\\&=0,\end{aligned} \quad (86)$$

which can be transformed into

$$p_k=\frac{(\eta-cm-\lambda_k)B}{(\varsigma/\varphi M+\mu)m\ln 2}-\frac{N_kB}{\delta_k\theta_k}. \quad (87)$$

Upon taking into account both (83) and (84), we have:

$$p_k=\min\left\{\frac{(\eta-cm)B}{(\varsigma/\varphi M+\mu)m\ln 2}-\frac{N_kB}{\delta_k\theta_k},p_{k\mathrm{M}}\right\}. \quad (88)$$

On the other hand, taking advantage of the velocity constraint in (17) results in

$$p_k\leq p_{k\mathrm{M}}=\frac{BN_k}{\delta_k\theta_k}\left\{\exp\left[\frac{\ln 2}{B}(mv_{\mathrm{M}}+q_k)\right]-1\right\}, \quad (89)$$

and substituting (89) into (88) gives rise to the power allocation (36), where the Lagrange multiplier is either $\mu=0$ or satisfies $\sum_{k=1}^{K}p_k-p_{\mathrm{M}}=0$ in terms of the third KKT condition in (85). Furthermore, substituting (36) into $v_k(p_k)=\frac{B}{m}\log_2\left(1+\frac{p_k\delta_k\theta_k}{BN_k}\right)-\frac{q_k}{m}$ yields the vehicular velocity (37).

Appendix F
Proof of Theorem 4

The theorem is proved by the method of contradiction. When the number of vehicles is $K=1$, it is straightforward to obtain $\eta_{\mathrm{S}}^*=p_{\mathrm{T}1}(\tilde{p}_1)/v_1(\tilde{p}_1)=\tilde{\eta}_1$. To proceed for $K>1$, we assume that the minimum system PVR of $k+1$ vehicles is given by

$$\eta_{\mathrm{s}}(k+1)=\frac{\sum_{i=1}^{k}p_{\mathrm{T}i}(\tilde{p}_i)+p_{\mathrm{T}k+1}(p_{k+1})}{\sum_{i=1}^{k}v_i(\tilde{p}_i)+v_{k+1}(p_{k+1})},\ 1\leq k<K-1. \quad (90)$$

If $p_{k+1}\neq\tilde{p}_{k+1}$, based on *Theorem 1*, we have

$$\eta_{k+1}=\frac{p_{\mathrm{T}k+1}(p_{k+1})}{v_{k+1}(p_{k+1})}>\tilde{\eta}_{k+1}=\frac{p_{\mathrm{T}k+1}(\tilde{p}_{k+1})}{v_{k+1}(\tilde{p}_{k+1})}, \quad (91)$$

and therefore the current system PVR satisfies

$$\eta_{\mathrm{s}}(k+1)>\tilde{\eta}_{\mathrm{s}}(k+1)=\frac{\sum_{i=1}^{k}p_{\mathrm{T}i}(\tilde{p}_i)+p_{\mathrm{T}k+1}(\tilde{p}_{k+1})}{\sum_{i=1}^{k}v_i(\tilde{p}_i)+v_{k+1}(\tilde{p}_{k+1})}, \quad (92)$$

which contradicts to the minimization criterion of the system PVR. Hence, the power allocation minimizing the system PVR is the same to that minimizing the vehicle PVR.

References

[1] M. Shafi, A. F. Molisch, P. J. Smith, T. Haustein, P. Zhu, P. D. Silva, F. Tufvesson, A. Benjebbour, and G. Wunder, "5G: A tutorial overview of standards, trials, challenges, deployment, and practice," *IEEE J. Sel. Areas Commun.*, vol. 35, no. 6, pp. 1201-1221, Apr. 2017.

[2] J. N. Ortiz, P. R. Diaz, S. Sendra, P. Ameigeiras, J. J. R. Munoz, and J. M. L. Soler, "A survey on 5G usage scenarios and traffic models," *IEEE Commun. Surveys Tuts.*, vol. 22, no. 2, pp. 905-929, Secondquarter, 2020.

[3] M. Giordani, M. Polese, M. Mezzavilla, S. Rangan, and M. Zorzi, "Towards 6G networks: Use cases and technologies," https://arxiv.org/abs/1903.12216.

[4] S. Chen, J. Hu, Y. Shi, L. Zhao, and W. Li, "A vision of C-V2X: Technologies, field testing and challenges with Chinese development," *IEEE Internet Things J.*, vol. 7, no. 5, pp. 3872-3881, Feb. 2020.

[5] 3GPP. TS38.885. Study on NR vehicle-to-everything (V2X), Mar. 2019.

[6] L. Liang, H. Peng, G. Y. Li, and X. Shen, "Vehicular communications: A physical layer perspective," *IEEE Trans. Veh. Technol.*, vol. 66, no. 12, pp. 10647-10659, Dec. 2017.

[7] S. Correia, A. Boukerche, and R. I. Meneguette, "An architecture for hierarchical software-defined vehicular networks," *IEEE Commun. Mag.*, vol. 55, no. 7, pp. 80-86, Jul. 2017.

[8] K. Zheng, L. Hou, H. Meng, Q. Zheng, N. Lu, and L. Lei, "Soft-defined heterogeneous vehicular network: Architecture and challenge," *IEEE Netw.*, vol. 30, no. 4, pp. 72-80, July 2016.

[9] W. Shi, H. Zhou, J. Li, W. Xu, N. Zhang, and X. Shen, "Drone assisted vehicular networks: Architecture, challenges and opportunities," *IEEE Netw.*, vol. 32, no. 3, pp. 130-137, May 2018.

[10] N. Zhang, S. Zhang, P. Yang, O. Alhussein, W. Zhuang, and X. Shen, "Software defined space-air-ground integrated vehicular networks: Challenges and solutions," *IEEE Commun. Mag.*, vol. 55, no. 7, pp. 101-109, Jul. 2017.

[11] L. Qian, Y. Wu, H. Zhou, and X. Shen, "Non-orthogonal multiple access vehicular small cell networks: Architecture and solution," *IEEE Netw.*, vol. 31, no. 4, pp. 15-21, Jul. 2017.

[12] Y. Liu, Z. Qin, M. Elkashlan, Z. Ding, A. Nallanathan, and L. Hanzo, "Nonorthogonal multiple access for 5G and beyond," *Proc. IEEE*, vol. 105, no. 12, pp. 2347-2381, Dec. 2017.

[13] L. Dai, B. Wang, Z. Ding, Z. Wang, S. Chen, and L. Hanzo, "A survey of non-orthogonal multiple access for 5G," *IEEE Commun. Surveys Tuts.*, vol. 20, no. 3, pp. 2294-2323, Thirdquarter, 2018.

[14] S. Fang, H. Chen, Z. Khan, and P. Fan, "On the content delivery efficiency of NOMA assisted vehicular communication networks with delay constraints," *IEEE Wireless Commun. Lett.*, vol. 9, no. 6, pp. 847-850, Jun. 2020.

[15] Z. Su, Y. Hui, Q. Xu, T. Yang, J. Liu, and Y. Jia, "An edge caching scheme to distribute content in vehicular netowrks," *IEEE Trans. Veh. Technol.*, vol. 67, no. 6, pp. 5346-5356, Jun. 2018.

[16] L. T. Tan, R. Q. Hu, and L. Hanzo, "Twin-timescale artificial intelligence aided mobility-aware edge caching and computing in vehicular networks," *IEEE Trans. Veh. Technol.*, vol. 68, no. 4, pp. 3086-3099, Apr. 2019.

[17] J. Chen, H. Wu, P. Yang, F. Lyu, and X. Shen, "Cooperative edge caching with location-based and popular contents for vehicular networks," *IEEE Trans. Veh. Technol.*, online publication, 2020.

[18] S. Sun, J. Hu, Y. Peng, X. Pan, L. Zhao, and J. Fang, "Support for vehicle-to-everything services based on LTE," *IEEE Wireless Commun.*, vol. 23, no. 3, pp. 4-8, Jun. 2016.

[19] M. Ivanov, F. Brannstrom, A. Amat, and P. Popovski, "Broadcast coded slotted ALOHA: A finite frame length analysis," *IEEE Trans. Commun.,* vol. 65, no. 2, pp. 651-662, Feb. 2017.

[20] Y. Sun, L. Xu, Y. Tang, and W. Zhuang, "Traffic offloading for online video service in vehicular networks: A cooperative approach," *IEEE Trans. Veh. Technol.*, vol. 67, no. 8, pp. 7630-7642, Aug. 2018.

[21] Q. Zheng, K. Zheng, L. Sun, and V. Leung, "Dynamic performance analysis of uplink transmission in cluster-based heterogeneous vehicular networks," *IEEE Trans. Veh. Technol.*, vol. 64, no. 12, pp. 5584-5595, Dec. 2015.

[22] J. Wang, Y. Huang, Z. Feng, C. Jiang, H. Zhang, and V. C. M. Leung, "Reliability traffic density estimation in vehicular network," *IEEE Trans. Veh. Technol.*, vol. 67, no. 7, pp. 6424-6437, Jul. 2018.

[23] N. Wisitpongphan, F. Bai, P. Mudalige, V. Sadekar, and O. Tonguz, "Routing in sparse vehicular Ad Hoc wireless networks," *IEEE J. Sel. Areas Commun.*, vol. 25, no. 8, pp. 1538-1556, Oct. 2007.

[24] A. Abdrabou and W. Zhuang, "Probabilistic delay control and road side unit placement for vehicular ad hoc networks with disrupted connectivity," *IEEE J. Sel. Area Commun.*, vol. 29, no. 1, pp. 129-139, Jan. 2011.

[25] H. Yang, K. Zheng, L. Zhao, and L. Hanzo, "Twin-timescale radio resource management for ultra-reliable and low-latency vehicular networks," *IEEE Trans. Veh. Technol.*, vol. 69, no. 1, pp. 1023-1036, Jan. 2020.

[26] M. J. Khabbaz, W. F. Fawaz, and C. M. Assi, "A simple free-flow traffic model for vehicular intermittently connected networks," *IEEE Trans. Intell. Transp. Syst.*, vol. 13, no. 3, pp. 1312-1326, Sep. 2012.

[27] X. Qu, E. Liu, R. Wang, and H. Ma, "Complex network analysis of VANET topology with realistic vehicular traces," *IEEE Trans. Veh. Technol.*, vol. 69, no. 4, pp. 4426-4438, Apr. 2020.

[28] J. Wang, C. Jiang, Z. Han, Y. Ren, and L. Hanzo, "Internet of vehicles: Sensing-aided transportation information collection and diffusion," *IEEE Trans. Veh. Techn.*, vol. 67, no. 5, pp. 3813-3825, May 2018.

[29] D. Feng, C. Jiang, G. Lim, L. J. Cimini, G. Feng, and G. Y. Li, "A survey of energy-efficient wireless communications," *IEEE Commun. Surveys Tuts.*, vol. 15, no. 1, pp. 167-178, First Quarter, 2013.

[30] M. D. Renzo, A. Zappone, T. T. Lam, and M. Debbah, "System level modeling and optimization of the energy efficiency in cellular networks-A stochastic geometry framework," *IEEE Trans. Wireless Commun.*, vol. 17, no. 4, pp. 2539-2556, Apr. 2018.

[31] C. Isheden, Z. Chong, E. Jorswieck, and G. Fettweis, "Framework for link-level energy efficiency optimization with informed transmitter," *IEEE Trans. Wireless Commun.*, vol. 11, no. 8, pp. 2946-2957, Aug. 2012.

[32] L. You, J. Xiong, X. Yi, J. Wang, W. Wang, and X. Gao, "Energy efficiency optimization for downlink massive MIMO with statistical CSIT," *IEEE Trans. Wireless Commun.*, vol. 19, no. 4, pp. 2684-2698, Apr. 2020.

[33] Y. Xin, D. Wang, J. Li, H. Zhu, J. Wang, and X. You, "Area spectral efficiency and area energy efficiency of massive MIMO cellular systems," *IEEE Trans. Veh. Technol.*, vol. 65, no. 5, pp. 3243-3254, May 2016.

[34] I. W. Ho, S. C. Chau, E. R. Magsino, and K. Jia, "Efficient 3D road map data exchange for intelligent vehicles in vehicular fog networks," *IEEE Trans. Veh. Techn.*, vol. 69, no. 3, pp. 3151-3165, Mar. 2020.

[35] J. Wang, J. Liu, and N. Kato, "Networking and communications in autonomous driving: A survey," *IEEE Commun. Surveys Tuts.*, vol. 21, no. 2, pp. 1243-1274, Secondquarter, 2019.

[36] T. L. Marzetta, "Noncooperative cellular wireless with unlimited numbers of base station antennas," *IEEE Trans. Wireless Commun.*, vol. 9, no. 11, pp. 3590-3600, Nov. 2010.

[37] S. Yan, R. Malaney, I. Nevat, and G. W. Peters, "Location verification systems for VANETs in Rician fading channels," *IEEE Trans. Veh. Technol.*, vol. 65, no. 7, pp. 5652-5664, Jul. 2016.

[38] S. Yan, R. Malaney, I. Nevat, and G. W. Peters, "Location spoofing detection for VANETs by a single base station in Rician fading channels," in *Proc. IEEE Veh. Technol. Conf.*, Glasgow, UK, May, 11-14, 2015, pp. 1-6.

[39] Z. Shen, K. Xu, and X. Xia, "Beam-domain anti-jamming transmission for downlink massive MIMO systems: A stackelberg game perspective," *IEEE Trans. Inf. Forensics Security*, online publication, 2021.

[40] Z. Shen, K. Xu, X. Xia, W. Xie, and D. Zhang, "Spatial sparsity based secure transmission strategy for massive MIMO systems against simultaneous jamming and eavesdropping," *IEEE Trans. Inf. Forensics Security*, vol. 15, pp. 3760-3774, Jun. 2020.

[41] L. Zhao, X. Wang, and K. Zheng, "Downlink hybrid information and energy transfer with massive MIMO," *IEEE Trans. Wireless Commun.*, vol. 15, no. 2, pp. 1309-1322, Feb. 2016.

[42] W. Xu, J. Liu, S. Jin, and X. Dong, "Spectral and energy efficiency of multi-pair massive MIMO relay network with hybrid processing," *IEEE Trans. Commun.*, vol. 65, no. 9, pp. 3794-3808, Sep. 2017.

[43] E. Björnson, E. G. Larsson, and T. L. Marzetta, "Massive MIMO: Ten myths and one critical question," *IEEE Commun. Mag.*, vol. 54, no. 2, pp. 114-123, Feb. 2016.

[44] E. Björnson, L. Sanguinetti, J. Hoydis, and M. Debbah, "Optimal design of energy-efficient multi-user MIMO systems: Is massive MIMO the answer?," *IEEE Trans. Wireless Commun.*, vol. 14, no. 6, pp. 3059-3075, June 2015.

[45] J. Xu and L. Qiu, "Energy efficiency optimization for MIMO broadcast channels," *IEEE Trans. Wireless Commun.*, vol. 12, no. 2, pp. 690-701, Feb. 2013.

[46] T. A. Khan, A. Yazdan, and R. W. Heath, "Optimization of power transfer efficiency and energy efficiency for wireless-powered systems with massive MIMO," *IEEE Trans. Wireless Commun.*, vol. 17, no. 11, pp. 7159-7172, Nov. 2018.

[47] L. Zhao, F. Wang, K. Zheng, and T. Riihonen, "Joint optimization of communication and traffic efficiency in vehicular networks," *IEEE Trans. Veh. Techn.*, vol. 68, no. 2, pp. 2014-2018, Feb. 2019.

[48] D. Ni, *Traffic Flow Theory: Characteristics, Experimental Methods, and Numerical Techniques*. Oxford, U.K.: Butterworth-Heinemann, Oct. 2015.

[49] H. Yu, H. D. Tuan, E. Dutkiewicz, H. V. Poor, and L. Hanzo, "Maximizing the geometric mean of user-rates to improve rate-fairness: Proper vs. improper Gaussian signaling," *IEEE Trans Wirel. Commun.*, online publication, 2021.

[50] R. M. Corless, G. H. Gonnet, D. E. G. Hare, et al., "On the Lambert W function," *Adv. Comput. Math.*, vol. 5, no. 1, pp. 329-359, Dec. 1996.

[51] M. Sadeghi, E. Björnson, E. G. Larsson, C. Yuen, and T. L. Marzetta, "Max-min fair transmit precoding for multi-group multicasting in massive MIMO," *IEEE Trans. Wireless Commun.*, vol. 17, no. 2, pp. 1358-1372, Feb. 2018.

[52] S. Boyd and L. Vandenberghe, *Convex Optimization*. Cambridge, U.K.: Cambridge Univ. Press, 2004.

[53] K. Shen and W. Yu, "Fractional programming for communication systems-part I: Power control and beamforming," *IEEE Trans. Signal Process.*, vol. 66, no. 10, pp. 2616-2630, May 2018.